Non-equivalent Pr^{3+} centres in $Gd_3Ga_{15}O_{12}$

1995 J. Phys.: Condens. Matter 7 5701

(http://iopscience.iop.org/0953-8984/7/28/022)

J. Phys.: Condens. Matter 7 (1995) 5701–5712. Printed in the UK

Non-equivalent Pr^{3+} centres in $Gd_3Ga_{15}O_{12}$

A Lupei†§, H Gross† and P Reiche‡

† Institute of Solid State Physics, Technical University of Darmstadt, 64289 Darmstadt, Germany

‡ Institute for Crystal Growing, Berlin-Adlershof, Germany

Received 9 February 1995, in final form 11 April 1995

Abstract. The Pr^{3+} spectra of $Gd_3Ga_5O_{12}$ Czochralski-grown crystals, investigated by absorption, site-selective excitation and emission and fluorescence decays, shows a complex structure. Besides the spectra assigned to Pr^{3+} in dodecahedral c sites (D_2 local symmetry), Pr^{3+} in other sites is also significant. An attempt to assign the most intense lines to structural defects is made. Three of the most intense satellite lines are assigned to a $Pr^{3+}(c)$ ion perturbed by a nearby non-stoichiometric defect (Gd^{3+} in octahedral a sites) whose concentration is estimated to be about 7%. The spectra for perturbed Pr^{3+} centres show additional lines connected with a reduction in local symmetry. Two other lines have been assigned to $Pr^{3+}(c)$–$Pr^{3+}(c)$ pairs. The $^3P_0$ emission decays are almost exponential with similar lifetimes, except one that presents a very strong quenching. This line has been assigned to strongly coupled $Pr^{3+}(c)$–$Pr^{3+}(c)$ nearest-neighbour pairs. The influence of pair quenching on the relative quantum efficiency of $^3P_0$ emission is also estimated.

1. Introduction

The spectroscopy of the $Pr^{3+}(4f^2)$ ion in various crystals has received increased attention in the last few years owing to the demonstration of the potentiality of these systems as laser active media [1–3] for visible emission. Spectral studies on Pr^{3+} in garnets refer especially to the determination of the energy level schemes of the main centre, i.e. Pr^{3+} in dodecahedral c sites of local D_2 symmetry [4, 5] and characteristics of up-conversion processes [6, 7].

The multisite structure of Pr^{3+} has also been investigated in $Y_3Al_5O_{12}$ (YAG) crystals [8, 9] and recently [10] in $Y_3Ga_5O_{12}$ (YGG). The studies on YAG refer to Czochralski-grown crystals; three different sites (including the main site) have been initially observed [8] and subsequently [9] a very complex structure has been reported in the analysis of the $^1D_2$ emission by pumping in higher Stark levels of the same multiplet. Two different environments have been found recently [10] in YGG Pr^{3+}, one of them being a minority site, having a very complex spectrum and assigned to a 'non-garnet' site of C_2 local symmetry. The elucidation of the Pr^{3+} multisite structure in garnets is important not only for the structural information that could be obtained but also since it might provide data on the Pr^{3+}–Pr^{3+} interactions, energy transfer processes including the up-conversion mechanisms, etc, as has been demonstrated for other rare-earth ions in garnets.

This paper reports the data concerning the Pr^{3+} multisite structure in $Gd_3Ga_5O_{12}$ (GGG), Czochralski-grown crystals. High-resolution transmission, integral excitation spectra, site-selective excitation and emission spectra and lifetime measurements have been performed

§ On leave from Institute of Atomic Physics, Bucharest 76900, Romania.

0953-8984/95/285701+12$19.50

at low temperatures. The analysis refers especially to the multisite structure of $^3P_1$ and $^3P_0$ and partially to $^1D_2$ multiplets. In the analysis of the data, previous results on the nature of the multisite structure of other RE^{3+} (RE = rare earth) ions in garnets have been taken into account. Thus, in high-temperature-grown (Czochralski or Bridgman) garnet crystals the RE^{3+} spectra could consist of the following [11].

(I) *The main lines N correspond to* RE^{3+} *in dodecahedral c sites of* D_2 *local symmetry.*

(II) The M lines correspond to various $RE^{3+}(c)$–$RE^{3+}(c)$ pairs; a concentration dependence of the M-to-N intensity rate and generally lower lifetimes than those for isolated RE^{3+} ions are expected.

(III) The P lines are observed mainly in high-temperature-grown (Czochralski or Bridgman) garnets. They consist of groups of satellites, whose number depends on spectral resolution, RE^{3+} ion, investigated transition or host garnet crystal. Up to three such lines have been reported for YAG:Er^{3+} and GGG:Er^{3+} [11] and YAG:Nd^{3+} [11, 12]. These lines have been assigned to RE^{3+} in *c* sites perturbed by a nearby non-stoichiometric defect (Y^{3+} or Gd^{3+} in octahedral *a* sites occupied normally by Al^{3+} or Ga^{3+}). Since this defect depends on the growth temperature (it is negligible in flux-grown garnets) and on the garnet type, the P-to-N ratio should depend on the crystal and not on the RE^{3+} concentration.

(IV) The A lines are assigned to RE^{3+} ions in octahedral sites (of C_{3i} local symmetry).

(V) Other satellite lines of lower intensities or irregular appearance are present, as was observed [12–14] for Tb^{3+}, Tm^{3+} or Nd^{3+} spectra in YAG.

2. Experiment

The GGG:Pr^{3+} single crystal with about 1 at.% Pr^{3+} was grown by the Czochralski method. It had edges cut along the [001], [110] and [1$\bar{1}$0] directions and polished to optical quality. The spectra were taken with the crystal immersed in liquid or gaseous helium. The fluorescence was excited with a nitrogen-laser[15]-pumped tunable dye laser (Lambda Physik, FL 2000) at a repetition rate of about 30 Hz. Spectral resolution was performed with a 3 m McPherson monochromator equipped with a grating with 1200 lines mm^{-1}. The fluorescence signal was detected by a photon-counting technique using a cooled photomultiplier (Hamamatsu R943-05) and a PC equipped with a multichannel-scalar board (EG%G, ACE-MCS). Absorption spectra were taken with a high-pressure xenon arc lamp.

3. Results

3.1. Transmission spectra

Pr^{3+} enters predominantly in dodecahedral $Gd^{3+}c$ sites of D_2 symmetry (centre N). The optical transitions between the Stark singlets characterized by the irreducible representations Γ_i of D_2 point group are governed by corresponding selection rules, with $\Gamma_i \rightarrow \Gamma_i$ forbidden transitions for both electric and magnetic dipoles. The position of the lowest Stark levels of the ground multiplet $^3H_4$ have been established from absorption and emission measurements and confirm the previous published data [5]. By polarized excitation and emission spectra, based on the technique developed in [13], we have been able to assign symmetry labels to several of them: *1(0 cm^{-1}), Γ_3; 2(20 cm^{-1}), Γ_1 and 3(37 cm^{-1}), Γ_4, if the local axes of* D_2 are defined as in [4].

The low-temperature transmission spectra corresponding to transitions from $^3H_4$ to $^3P_0(\Gamma_1)$ and $^3P_1(\Gamma_2, \Gamma_3, \Gamma_4)$ are shown in figure 1(*a*) and figure 2(*a*). They contain one

and two main lines N^i, respectively, the superscript denoting the Stark levels in increasing energy order. The Stark energy levels of the $^3P_1$ multiplet and their symmetry labels, as given in table 1 (centre N), have been established using the selective polarized excitation and emission technique [13] and using the hot band structure of absorption and excitation spectra as in [5]. The position of the level Γ_3 is different from previous assignments [4, 5]. The absorption spectra $^3H_4(\Gamma_3) \rightarrow {}^1D_2(\Gamma_1, \Gamma_2, \Gamma_1, \Gamma_3, \Gamma_4)$ present four N^i lines as allowed by selection rules. Two of them, corresponding to transitions $^3H_4(\Gamma_3) \rightarrow {}^1D_2(\Gamma_1, \Gamma_2)$ to the lowest Stark components of $^1D_2$, are shown in figure 3. The symmetry labels for the $^1D_2$ Stark components have been established by the same techniques [4, 13]. Besides these N lines, associated with allowed transitions from the $^3H_4(\Gamma_3)$ ground-state level, the very-low-temperature transmission spectra contain a series of satellites, which are less resolved especially in the lines corresponding to transitions to higher Stark levels of $^1D_2$. At high temperatures, hot bands are also observed.

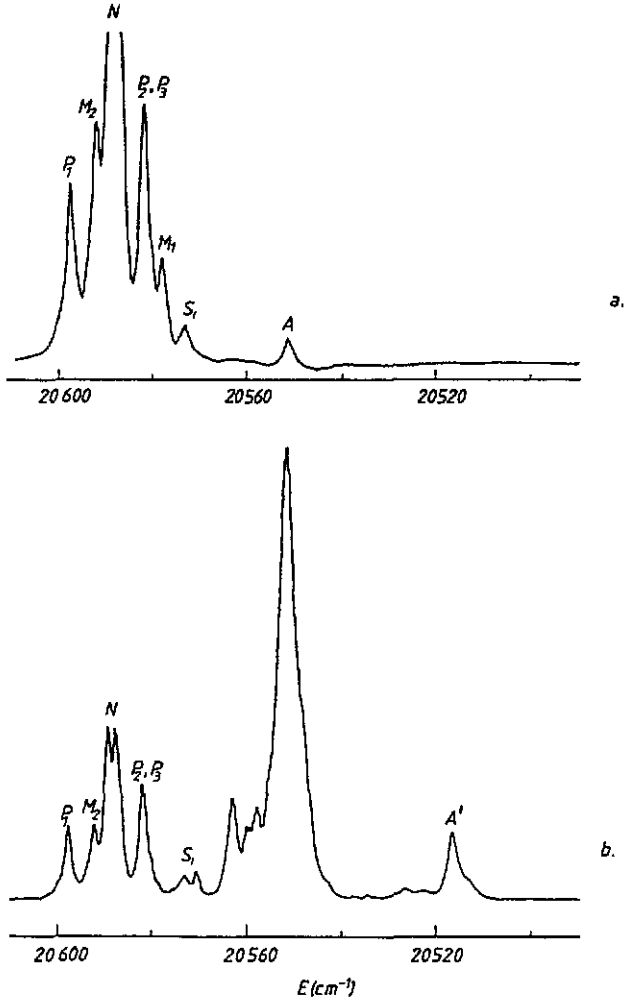

Figure 1. Transmission spectrum at 4.2 K of (*a*) the $^3H_4 \rightarrow {}^3P_0$ transition and (*b*) partial $^3P_0 \rightarrow {}^3H_4$ emission on non-selective pumping.

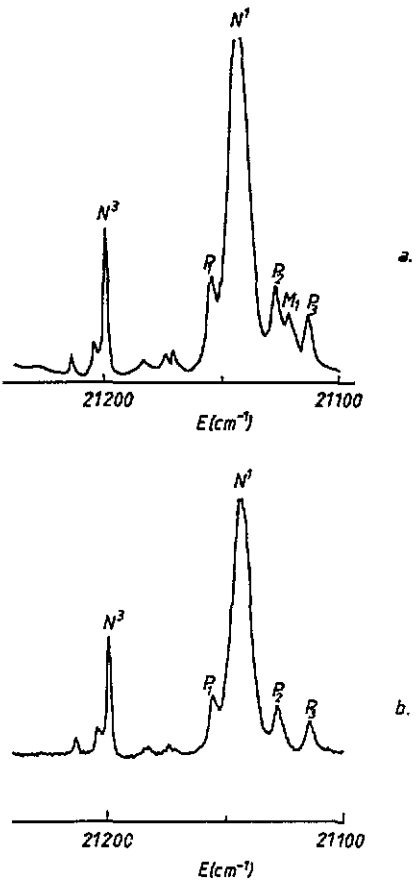

Figure 2. (*a*) Transmission spectrum for $^3H_4 \rightarrow {}^3P_1$ and (*b*) integral excitation spectrum of $^3P_0$ and $^1D_2$ emission in the same region excited at 4.2 K.

Table 1. Stark energy levels of main non-equivalent Pr^{3+} centres in GGG in $^3P_0$ and $^3P_1$ multiplets.

Centre	$^3P_0$ (cm^{-1})	$^3P_1$ (cm^{-1})		
N	20589 (Γ_1)	21141 (Γ_2)	21188 (Γ_3)	21198 (Γ_4)
P_1	20597.5	21153	21181	21213
M_2	20592.5	21147	21183	21200
P_2	20582	21126	21174	21198
P_3	20581	21112	21154	21198
M_1	20578.5	21120	—	—
S_1	20573.5	21106	21132	21172
S_2	20571	21098	21154	21225
A	20551	21112	—	—

The satellite structure connected with the $^3H_4(\Gamma_3) \rightarrow {}^3P_0(\Gamma_1)$ transition (figure 1(*a*)) could be separated into two groups: four rather intense lines (denoted P_i and M_i, for arguments which will be given later) within ± 10 cm^{-1} from the main line N and others less

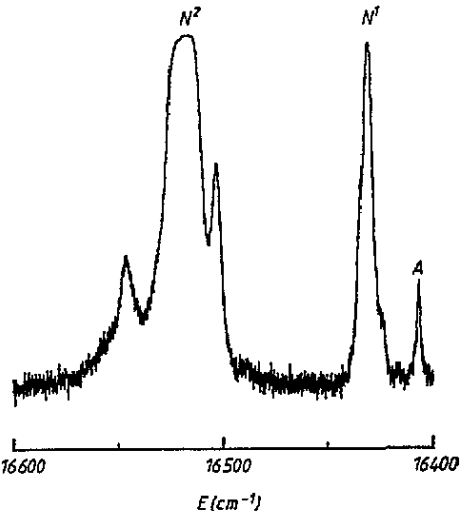

Figure 3. Part of the transmission spectrum corresponding to the $^3H_4 \rightarrow {}^1D_2$ transition at 4.2 K.

intense and more shifted lines (S_i and A). The intensity of the A line is possibly enhanced by a superimposed hot band, but it has been observed at 1.6 K, too. The second derivative of the absorption spectrum in figure 1(*a*) suggests the superposition of two almost equally intense lines P_2 and P_3, a fact demonstrated by site-selective excitation and emission.

Besides the satellite structure concentrated near the main lines N^1 and N^3, corresponding to the allowed $^3H_4(\Gamma_3) \rightarrow {}^3P_1(\Gamma_2, \Gamma_4)$ transitions (figure 2(*a*)) a series of satellite lines between them should be noted. As the high-temperature transmission and the selective excitation spectra have shown, this structure is connected to the forbidden $^3H_4(\Gamma_3) \rightarrow {}^3P_1(\Gamma_3)$ (see table 1) transition for D_2 local symmetry; the N line for this transition is missing. In the $^3H_4 \rightarrow {}^3P_1$ transition near the N^1 line, three satellites of almost equal intensity (see also the integral excitation spectrum in figure 2(*b*)) could be assigned to P-type lines.

The resolution of the satellite structure in absorption for the transitions to $^1D_2$ is less clear than that for $^3P_0$ and $^3P_1$. It is relatively good only for the first two Stark levels (figure 3); as a feature of this transition the rather intense line denoted A, shifted by about -25 cm^{-1} from the main line N^1, should also be noted.

3.2. Selective excitation and emission spectra

The excitation spectrum of the integral $^3P_0$ and $^1D_2$ emissions in the $^3P_1$ absorption region is presented in figure 2(*b*). It reflects with one exception (the M_1 line that is missing) the main features of the transmission spectra. The relative intensities of the main lines and satellites are affected by strong absorption of the laser by the main lines N and reabsorption of the emitted light; these effects have been used in the selective excitation measurements for a better resolution of the satellites. Part of the $^3P_0 \rightarrow {}^3H_4$ emission at non-selective pumping (see below) is illustrated in figure 1(*b*). It shows in the region of the $^3P_0(\Gamma_1) \rightarrow {}^3H_4(\Gamma_3)$ transition the same lines as the corresponding absorption (figure 1(*a*)), except for the M_1 line. Lines corresponding to the $^3P_0(\Gamma_1) \rightarrow {}^3H_4(\Gamma_4)$ transitions to the third Stark level of $^3H_4$ are also observed. The reabsorption of the main line N and the line A′ most shifted

towards lower energies, which corresponds to the $^3P_0 \rightarrow {}^3H_4(3)$ transition of centre A, should be noted.

Since GGG has large phonons, the excitation from $^3P_1$ is transmitted to $^3P_0$ by a fast non-radiative decay. The $^3P_1$ excitation spectra of satellite lines observed in the $^3P_0$ absorption are generally different from that of the N line, as illustrated in figure 4 (the intensity scales are not the same and some non-selectivity is also present). The $^3P_1$ excitation spectrum of $^3P_0$ N emission contains two lines (figure 4(*a*)) corresponding to the N^1 and N^3 absorption lines from figure 1(*a*). A characteristic of the excitation spectra of some satellites (P_i and S_i) in comparison with that of N is, besides the spectral shifts, the presence of a third line, and variations in the relative intensities of the three lines. The spectrum in figure 4(*d*) suggests a superposition of two lines P_2 and P_3 in $^3P_0$ absorption, a fact proved by emission spectra too. Almost no emission was observed (under our experimental conditions), at the wavelength of the M_1 line by tuning the excitation laser over the whole range of the $^3P_1$ absorption (figure 4(*e*)). Pumping in the broad and very weak excitation lines (figure 4(*e*)) leads to a non-selective emission of $^3P_0$ which, however does not contain M_1. The absence of any line in the excitation spectrum related to the M_1 line could be explained by a strong fluorescence quenching which reduces its lifetime under the temporal resolution of our set-up, a fact already observed for near-neighbour pairs of Nd^{3+} in YAG [11, 12]. The excitation spectra of S_i satellites indicate the presence of at least two strongly distorted centres. A very peculiar behaviour is shown in the excitation spectrum (figure 4(*g*)) of the A centre (the same by detection of either the $^3P_0$ or the $^1D_2$ emissions). It is quite different from those of all other centres.

The crystal-field components of the $^3P_0$ and $^3P_1$ levels for various structural centres of Pr^{3+} in GGG as determined from transmission, emission and excitation spectra are given in table 1. The determination of positions for all Stark components of the $^3H_4$ multiplet was not possible, since the emission spectra for the higher components contain a large number of lines possibly due to vibronic transitions [8]. The $^1D_2$ emission due to pumping in $^3P_1$ has also been investigated. The spectral selectivity in this case is partially lost; a characteristic of the spectra is that, besides the excited satellite line, they contain in various proportions contributions of N and A centres and the decays show rise times. This behaviour needs further investigation.

The $^3P_0$ emission kinetics at 4.2 K show nearly exponential decays with similar lifetimes of 15.5–18.5 μs for almost all lines including N whose lifetime is longest, about 18.5 μs. The exception is the M_1 line whose decay must be very fast, faster than the resolution (2 μs) of our set-up. Owing to the short lifetime of the $^3P_0$ level and possible contribution of the main line, one cannot give precise values for the lifetimes of every satellite. At the beginning of the decays (up to 20 μs), values of 17–18 μs have been measured for the P_i lines, and about 15.5 μs for the M_2 line. The decay of the A line is almost exponential with a lifetime of about 16 μs.

At selective pumping in $^3P_1$ the $^1D_2$ emission decays present a rise time corresponding to the lifetime of $^3P_0$, suggesting a population by non-radiative de-excitation, followed by decays with lifetimes varying between 260 μs for N and 200 μs for the A centre, which is the most isolated line and can be precisely determined.

4. Discussion

The previous studies concerning the Pr^{3+} multisite structure in garnets refer especially to YAG and are limited to describing the spectral characteristics of various non-equivalent sites.

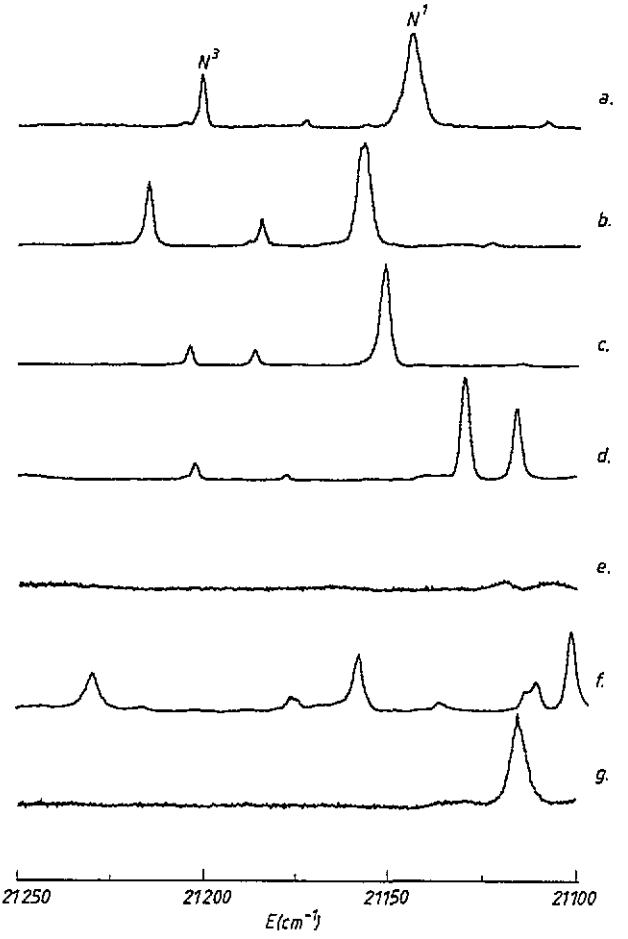

Figure 4. Selective excitation spectra (at 4.2 K) of various $^3P_0 \rightarrow {}^3H_4$ emission lines in the region of the $^3H_4(\Gamma_3) \rightarrow {}^3P_1$ absorption: (*a*) N; (*b*) P_1; (*c*) M_2; (*d*) P_2 and P_3; (*e*) M_1; (*f*) S_t; (*g*) A.

In this report an attempt is made to connect the non-equivalent sites of Pr^{3+} in GGG (not reported to our knowledge before) to structural data. The observed satellite structure in GGG:Pr^{3+} is intrinsic to the system, since it has been observed in many transitions of the Pr^{3+} ion. The ionic radii of Pr^{3+} are close to those of Nd^{3+}; therefore one should expect similar non-equivalent sites to those observed for YAG:Nd^{3+} [11, 12], i.e. mainly pairs and perturbed centres due to non-stoichiometric defects (according to previous data [11], the latter occur in a larger concentration in GGG than in YAG).

Since in eightfold coordination the ionic radius of Pr^{3+} (1.14 Å) is larger than that of Gd^{3+} (1.06 Å), the changes in the crystal field produced by the mutual influence of two close Pr^{3+} ions in *c* sites are expected to be quite large and various pairs should show up as shifted lines in high-resolution spectra. The RE^{3+} distribution in garnets is random so that the probability of pair formation is finite, even at low concentrations. The assignment of M_1 lines to $Pr^{3+}(c)$–$Pr^{3+}(c)$ nearest-neighbour pairs at 3.79 Å is very likely. The quenching of M_1 $^3P_0$ emission could be produced by a strong short-range ion–ion interaction, most probably superexchange. A satellite line whose intensity increases

quadratically with increasing Pr^{3+} concentration and has a very short lifetime (about 1 μs) has been also observed in the $^1D_2$ emission of Pr^{3+} in YAG [9]. In the garnet structure, two close RE^{3+} in c sites have bonds via oxygen bridges with an angle of about 100°, and thus the superexchange interaction between them is possible. This is no longer valid for the next neighbours situated at 5.79 Å. Evidence of Pr^{3+} pairs coupled by superexchange interaction has also been reported for LaF_3 [16] and $LiYF_4$ [17]. A strongly coupled pairs model has also been proposed in [18] to explain the behaviour of Pr^{3+} pairs in $CsCdBr_3$. Although no significant quenching has been observed for the other Pr^{3+} emission lines of $^3P_0$ in GGG, from the analysis of the spectra and from the comparison with YAG:Nd^{3+} [12], one can assume that some of the other satellites close to main lines could be connected with other $Pr^{3+}(c)$–$Pr^{3+}(c)$ pairs. Thus, M_2 lines observed in spectra connected with $^3P_0$ and $^3P_1$ multiplets could be related to $Pr^{3+}(c)$–$Pr^{3+}(c)$ next-nearest pairs at 5.79 Å. Such a pair with fluorescence quenching due to a dipole–dipole interaction has been observed recently for Nd^{3+} in YAG [12] but, unlike Nd^{3+}, Pr^{3+} $^3P_0$ level emission as observed in various crystals [16, 19, 20] does not present significant concentration quenching at relatively low concentrations. By examining the general energy level scheme of Pr^{3+} in GGG [5], the most probable cross relaxation for $^3P_0$ fluorescence is

$$(^3P_0 \rightarrow {}^1G_4) + (^3H_4 \rightarrow {}^1G_4) \tag{1}$$

but only assisted by phonons (figure 5). At the same time, $^3H_4 \rightarrow {}^1G_4$ absorption and $^3P_0 \rightarrow {}^1G_4$ emission lines have very low intensities, both transitions being spin forbidden. Therefore this cross relaxation process is expected to be inefficient for distant $Pr^{3+}(c)$ ions coupled by multipolar interactions, the transfer rates W_i relatively small and the measured lifetimes τ_i for these pairs given by

$$\frac{1}{\tau_i} = W_i + \frac{1}{\tau_0} \tag{2}$$

would be close to the isolated ion lifetime τ_0. Therefore, one could have shifted pair lines, if the RE^{3+} ion is large compared with the host ion replaced without a significant change in the pair lifetime compared with that of isolated ions, if the emitting level is not involved in an effective cross relaxation. The situation is different for the nearest neighbours (lines M_1) for which one can estimate a lower limit for the transfer rate $W_1 < 4 \times 10^5$ s^{-1}. A strong short-range interaction (such as superexchange) could give such large transfer rates. An alternative mechanism that could contribute to a fast de-excitation of the strongly coupled pairs could be an enhanced multiphonon relaxation between the close-lying energy levels of the pair. If the resolution of the experimental set-up is low, such pairs cannot be observed and their contribution to the integral fluorescence quenching could be neglected. However, it should be considered when the quantum efficiency is estimated as has been discussed for YAG:Nd^{3+} [21].

Other energy transfer mechanisms for $^3P_0$ emission time behaviour of Pr^{3+} in YAG, at high temperatures, have been recently proposed [26]; a forward process $(^3P_0 \rightarrow {}^3H_6(8)) + (^3H_4(5) \rightarrow {}^1D_2(1))$ with an activation energy of 533 cm^{-1} and a backward process $(^1D_2(1) \rightarrow {}^3H_4(2)) + (^3H_6(9) \rightarrow {}^3P_1(2))$ with an activation energy of 431 cm^{-1}. This process needs further consideration since it assumes a lifetime for the $^3H_6$ level in the millisecond region (too large for a gap of only about 2000 cm^{-1} to the $^3H_5$ Pr^{3+} level in YAG) and involves forbidden transitions, if the symmetry label assignments in [4] are correct.

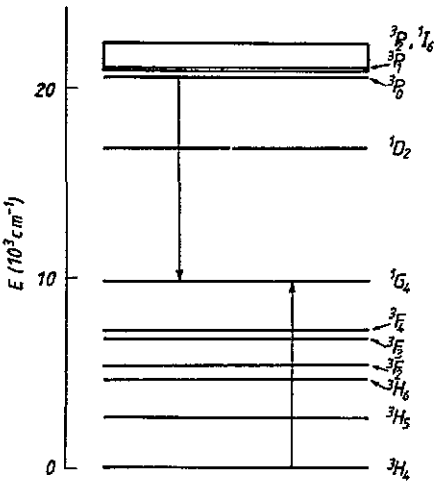

Figure 5. Energy level diagram of Pr^{3+} in GGG and schematic diagram for $^3P_0$ fluorescence quenching.

A very likely source of losses for $^3P_0$ main centre emission in GGG is a transfer to the A centre by a direct transfer process $(^3P_0 \rightarrow {}^3H_4(3))_N + (^3H_4(1) \rightarrow {}^3P_0)_A$ that is resonant and it is effective even at very low temperatures. This way one can explain the observation of the A line in $^1D_2$ emission, where it is isolated, even at non-selective pumping. The maximum of the $^1D_2$ emission for the A line at about 40 μs after the exciting laser pulse compared with about 55 μs for N lines suggests that this transfer takes place indeed in the upper $^3P_0$ level. A further investigation on samples with different Pr^{3+} concentrations would be necessary to clarify the contribution of this effect to the total quenching, since A centres represent only a few percent of the total Pr^{3+} ions. Migration on donors could increase the efficiency of this process.

The analysis of $^3P_0$ global decay is difficult since one should keep in mind several facts: the satellite structure, which is non-negligible in GGG, and therefore the system is inhomogeneous at low temperatures; the perturbed centres which have slightly lower lifetimes; strong absorption and reabsorption effects which increase with increasing concentration and affect the emission decay of the main centre no matter which luminescence is monitored.

One could, however, estimate the effect of pair quenching on the integral $^3P_0$ fluorescence kinetics (if the emission of the whole system is monitored). For a random uniform distribution of acceptors, the donor fluorescence kinetics can be written as [19, 22]

$$\frac{I}{I_0} = \exp\left(-\frac{t}{\tau_0}\right) \prod_i [1 - C_A + C_A \exp(-tW_i)] \tag{3}$$

where the product describing the energy transfer contribution extends over all i sites available to the acceptors, C_A is the relative acceptor concentration (which is equal to the Pr^{3+} concentration in this case) and W_i is the transfer rate corresponding to the acceptor at the site i. If the transfer rates for $i > 4$ are negligible ($W_i \simeq 0$), the product (3) is limited to the four near neighbours at 3.79 Å. The integral decay presents therefore at the beginning a time-dependent energy transfer contribution from nearest-neighbour pairs, which is a function of transfer rate W_1 and concentration C_A. This contribution is limited

at times of the order of $1/W_1$. For $t \gg 1/W_1$ the integral decay (3) becomes

$$\frac{I}{I_0} = \exp\left(-\frac{t}{\tau_0}\right)(1 - C_A)^4. \tag{4}$$

Therefore, at long times the decay is exponential with a lifetime τ_0, but it presents a uniform concentration-dependent reduction in intensity. If the time resolution t_r of the experimental set-up is low, e.g. $1/W_1 \gg t_r$, the integral fluorescence decay (3) can be also approximated by (4) and shows up as a normal exponential decay, the fast drop at the beginning not being observed.

The quenching due to nearest-neighbour pairs would reduce the quantum efficiency. By using equation (4), one could estimate a higher limit of the relative quantum efficiency (i.e. its reduction due only to the concentration quenching effects of nearest-neighbour pairs) as

$$\eta_r = (1 - C_A)^4. \tag{5}$$

For low concentrations, as used in Pr^{3+}-doped garnets as laser systems, $\eta_r \simeq 1 - 4C_A$. This approach is valid for all garnets at relatively low Pr^{3+} contents. At high concentrations the contribution of multipolar interactions could be larger and the quenching due to more distant acceptors non-negligible.

The $^1D_2$ level is involved in more effective cross relaxations that lead to its fluorescence concentration quenching, as the measurements on various crystals [9, 16, 17, 19] have shown. A satellite line whose intensity increases quadratically with increasing Pr^{3+} concentration and has a very short lifetime (about 1 μs) was detected in the $^1D_2$ emission of Pr^{3+} in YAG [9] and tentatively assigned to the nearest-neighbour pairs. In our experimental conditions we have not been able to detect pair lines at this level; the satellite structure is less clear and the selectivity is partially lost.

The three P_i satellites could be assigned to $Pr^{3+}(c)$–$Gd^{3+}(a)$ 'pairs', the perturbator Gd^{3+} in octahedral a sites being a non-stoichiometric defect demonstrated by different methods, including directly by EXAFS [23], where Gd^{3+}–O^{2-} distances corresponding to the octahedral vicinity have been measured. Arguments that a $Gd^{3+}(a)$ defect could lead to three different perturbations have been given in several papers [11, 12]. The hot band structure of the main centre N in absorption as well as in excitation spectra has allowed us to determine the position of the second $^3P_1$ Stark level of Γ_3 symmetry (table 1). This assignment is different from previous assignments for Pr^{3+} in YAG [4] or GGG [5]. The excitation spectra of some satellites, including P_i, contain a third line between N^1 and N^3 in the region where the line corresponding to the forbidden transition $^3H_4(\Gamma_3) \rightarrow {}^3P_1(\Gamma_3)$ in D_2 should be placed. The additional lines can be interpreted as a transition forbidden in D_2 but which is forced by a proper symmetry reduction for the given satellite centre so that $\Gamma_i \rightarrow \Gamma_i$ transitions become allowed. In fact for any subgroup of D_2 all the transitions are allowed.

The reduction in the symmetry of GGG from cubic to a lower symmetry has been suggested earlier from x-ray measurements [24]. Our x-ray data on YAG [12] or GGG show indeed very-low-intensity {222} reflections forbidden in cubic $Ia3d$ space group of the garnets, but they do not show any preferential [111] direction as assumed in [23, 24]. This indicates that the symmetry reduction is local and is due to randomly distributed defects in the {222} planes normally occupied by $Ga^{3+}(a)$ ions. These defects are very probably $Gd^{3+}(a)$ ions. Therefore, there is a connection between x-ray data that contain additional reflections and optical data that present shifted lines for allowed transition and for non-Kramers ions, even additional lines corresponding to $\Gamma_i \rightarrow \Gamma_i$ transitions forbidden in ideal

garnets. The P-to-N intensity ratio for one satellite, estimated from our transmission spectra, is about 10%; this value leads (assuming that $Gd^{3+}(a)$ is randomly distributed in the lattice and that one such defect determines three lines of equal intensity, as seen clearly in figure 2) to a concentration of Gd^{3+} ions in octahedral *a* sites of the order of 7%, a value similar to estimations from other RE^{3+} spectra in GGG [11].

It is difficult to assign the S_i lines. The emission and excitation spectra suggest a resemblance to the main centre, i.e. they behave like Pr^{3+} in *c* sites, but strongly distorted. One can assume that they result from $Pr^{3+}(c)$ by a local distortion introduced by some impurities or lattice defects. The centre giving A lines shows quite peculiar spectral characteristics: large shifts from N lines, strong absorption and emission in $^3H_4 \leftrightarrow {}^1D_2$ transition; quite a different excitation spectrum corresponding to the $^3P_1$ level which contains almost only one line (figure 4(*g*)); faster lifetimes than N for both $^3P_0$ and $^1D_2$ emissions. A tentative model for this centre which acts as a trap for the $^3P_0$ emission of the main centre would be Pr^{3+} in a Ga^{3+} *a* octahedral site. In undistorted octahedral C_{3i} symmetry, the magnetic dipole transitions should dominate the spectra. The analysed transitions do not satisfy the magnetic dipole selection rules $\Delta J = 0, \pm 1$. However, owing to the large ionic radii difference (Pr^{3+} in sixfold coordination has a radius of 1 Å, while Ga^{3+} a radius of only 0.62 Å), one could expect a lowering of the symmetry from C_{3i}, leading to electric dipole transitions and to a slight reduction in lifetimes. As has been demonstrated in [25] such a replacement is possible even for ions with large differences in ionic radii, but in a small concentration.

5. Conclusions

We have analysed the multisite structure of Pr^{3+} in GGG single crystals which were Czochralski grown, by using transmission, selective excitation and emission spectra. As the spectra have shown (figures 1–4) the structure connected with Pr^{3+} non-equivalent sites cannot be neglected in these crystals. The resonant $^3H_4 \leftrightarrow {}^3P_0$, $^3P_1$ transitions have been especially analysed. Three satellites P_i have been connected with a non-stoichiometric defect namely Gd^{3+} in octahedral *a* sites, which causes a reduction in the local symmetry of the Pr^{3+} ions demonstrated by spectroscopic and x-ray data. The concentration of this defect was estimated to be about 7%, compared with YAG where the concentration is only about 2%. A reduction in local symmetry is manifested by additional lines which correspond to forbidden transitions in D_2. In the limit of experimental errors the $^3P_0$ emission lifetimes of these lines at low temperatures are in the range 17–18.5 μs, close to that of the main line. The reduction in the lifetimes of the P_i centres could be due either to the energy transfer to the main centre or to static perturbations of the crystal fields. Two other sites M_i have been assigned to $Pr^{3+}(c)$–$Pr^{3+}(c)$ pairs: M_1 corresponding to nearest neighbours and showing a very strong quenching of $^3P_0$ luminescence; M_2, which shows a small quenching. These data are explained by the inefficient cross relaxations for $^3P_0$ level which could be overcome only by a very strong ion–ion interaction such as superexchange that couples only the near neighbours. The effect of pair quenching on the relative quantum efficiency is also discussed. One cannot assign definite structural models to some of the less intense lines (S_i and A). Owing to the similarities of S_i spectra with those of Pr^{3+} in the *c* site, one can assume that they result from a local distortion introduced by some impurities or lattice defects. A suggestion is made that the A centre could be connected with Pr^{3+} in octahedral Ga^{3+} sites, and an efficient N $\rightarrow$ A transfer is very likely.

Acknowledgments

A Lupei would like to thank the DAAD, Germany, for supporting her as a visiting scientist in Darmstadt. The authors express their gratitude to Professor J Heber for his fruitful discussions and revision of this paper and Dr C Stoicescu for x-ray measurements.

References

[1] Esterowitz L, Allen R, Kruer M, Bertoli F, Goldberg L S, Jenssen H P, Linz A and Nicolai V O 1977 *J. Appl. Phys.* **48** 650
[2] Bleckmann A, Heine F, Meyen J P, Petermann K and Huber G 1993 *OSA Proc. Adv. Solid State Lasers* A **TuB 1** 164–5
[3] Malinowski M, Joubert M F and Jacquier B 1993 *Phys. Status Solidi* a **140** K49
[4] Gruber J B, Hills M E, Macfarlane R M, Morrison C A and Turner G A 1989 *Chem. Phys.* **134** 241
[5] Antic-Fidancev E, Holsa J, Krupa J C, Lemaitre-Blaise M and Porcher P 1992 *J. Phys.: Condens. Matter* **4** 8321
[6] Capobianco J A, Raspa N, Monteil A and Malinowski M 1993 *J. Phys.: Condens. Matter* **5** 6083
[7] Malinowski M, Joubert M F and Jacquier B 1994 *J. Lumin.* **60–1** 179
[8] Antic-Fidancev E, Lemaitre-Blaise M, Krupa J C and Caro P 1988 *Czech. J. Phys.* B **38** 1269
[9] Malinowski M, Szczepanski P, Wolinski W, Wolski R and Frukacz Z 1993 *J. Phys.: Condens. Matter* **5** 6469
[10] Antic-Fidancev E, Lemaitre-Blaise M and Porcher P 1994 *J. Alloys Compounds* **207–8** 90
[11] Osiko V V, Voronko Yu K and Sobol A A 1974 *Crystal* vol 10 (Berlin: Springer) p 37
[12] Lupei V, Lupei A, Tiseanu C, Georgescu S, Stoicescu C and Nanau P M 1995 *Phys. Rev.* B **51** 8
[13] Bayerer R, Heber J and Mateika D 1986 *Z. Phys.* B **64** 201
[14] Lupei V, Lupei A and Boulon G 1994 *J. Physique* IV **4** 407
[15] Neukum J, Heber J, Haschka H J, Umhofel-Strobl U and Tang Xiao 1992 *Meas. Sci. Technol.* **3** 1198
[16] Vial J C and Buisson R 1982 *J. Physique Lett.* **43** L745
[17] Barthem R B, Buisson R and Vial J C 1987 *J. Lumin.* **38** 190
[18] Schafer U, Neukum J, Bodenchartz N and Heber J 1994 *J. Lumin.* **60–1** 633
[19] Dornauf H and Heber J 1980 *J. Lumin.* **22** 1
[20] Moriotto G, Tietz F, Zanghellini E and Ferrari M 1994 *J. Lumin.* **60–1** 216
[21] Lupei V, Lupei A, Georgescu S and Yen W M 1989 *J. Appl. Phys.* **66** 3792
[22] Golubov I S and Konobeev Yu V 1972 *Sov. Phys.–Solid State* **13** 2679
[23] Jun Dong and Kunquan Lu 1991 *Phys. Rev.* B **43** 8808
[24] Chenavas J, Joubert J C and Marezio M 1978 *J. Less-Common Met.* **62** 373
[25] Geller S, Espinosa G P, Fullmer L D and Crandall P B 1972 *Mater. Res. Bull.* **7** 1219
[26] Wu Xingkun, Dennis W M and Yen W M 1994 *Phys. Rev.* B **50** 6589